Recycled oceanic crust-derived fluids in the lithospheric mantle of eastern China: constraints from oxygen isotope compositions of peridotite xenoliths

Yantao Hao[1,3], Qunke Xia[1]*, Luigi Dallai[2], Massimo Coltorti[3]

1 CAS Key Laboratory of Crust-Mantle Materials and Environments, School of Earth and Space Sciences, University of Science and Technology of China, Hefei, 230026, China

2 CNR-Istituto di Geoscienze e Georisorse, Via G. Moruzzi 1, 56124, Pisa, Italy

3 Department of Earth Sciences, Ferrara University, Corso Ercole I d'Este, 32, 44100, Ferrara, Italy

*Corresponding author: qkxia@ustc.edu.cn

ABSTRACT

The oxygen isotope compositions of minerals of peridotite xenoliths from the Subei basin, Eastern China were investigated to detect a possible crustal signature in mantle rocks. The $\delta^{18}O$ values of olivine (ol), orthopyroxene (opx) and clinopyroxene (cpx) vary from 5.02 to 5.98‰, 5.46 to 6.78‰, and 4.37 to 6.31‰, respectively. Olivine and opx have $\delta^{18}O$ values similar to-, or above the "expected" mantle range, whereas the $\delta^{18}O$ values of cpx range from higher to lower than average mantle. These characteristics are inherited from the peridotite mantle source, and likely result from mantle domains that experienced fluid-assisted metasomatism. Coexisting high $\delta^{18}O$ values of ol and opx and low $\delta^{18}O$ values of cpx are unlikely to result from selective interactions with the fluids with different $\delta^{18}O$ values during a single metasomatic event. The variable rare earth elements (REE) concentrations of clinopyroxenes also indicate a multi-stage metasomatic history of the Subei mantle. The measured O-isotope values can be reconciled with a simplified two-stage metasomatic model characterized by an early high-$\delta^{18}O$ fluid/peridotite interaction followed by a late

28 low-δ^{18}O fluids infiltration. Model calculations of mineral diffusivities predict that the

29 negative $\Delta^{18}O_{cpx-ol}$ values are unlikely to be preserved at mantle conditions for time

30 interval > 100 Ma. Provided the investigated mantle xenoliths were entrained and

31 brought to surface by ~9 Ma basaltic eruptions, this also the limit for the occurrence

32 of the late metasomatic event(s), and the subducting Pacific plate is considered the

33 best candidate to provide such fluids.

34

35 **1. INTRODUCTION**

36   Tracing recycled crustal signatures is fundamental to understanding the chemical

37 complexity of the Earth's mantle. In addition, subduction-related fluids (here is a wide

38 definition, including fluids and melts) have shown to be tightly related to arc

39 magmatism [e.g. *Stolper and Newman,* 1994] and even intraplate magmatism [e.g.

40 *Kuritani et al.,* 2011]. Large fractionations at the near-surface conditions generate

41 prominent difference of oxygen isotope compositions between crustal and mantle

42 materials, making oxygen isotope a sensitive tool to recognize recycled crustal

43 signature from mantle-derived rocks and minerals.

44   The lithospheric mantle represented by peridotite xenoliths beneath eastern China

45 exhibit variable elemental and isotopic compositions which have been attributed to

46 multistage fluid-peridotite interactions (i.e. mantle metasomatism) [e.g. *Tatsumoto et*

47 *al.,* 1992; *Xu et al.,* 1996; *Xu et al.,* 2000; *Xu,* 2001; *Zheng et al.,* 1998, 2006; *Wu et*

48 *al.*, 2006; *Zhang et al.*, 2005; *Choi et al.*, 2008; *Tang et al.*, 2011]. Since early

49 Paleozoic time, eastern China had experienced multistage subduction of several

50   oceanic and continental plates and the Pacific plate is still subducting [e.g. *Windley et*

51   *al.*, 2010]. Crust-derived fluids therefore should be expected to be involved in

52   metasomatism occurred in eastern China, but the evidence has been scarce [e.g. *Xia et*

53   *al.*, 2004; *Su et al.*, 2011]. Moreover, widely distributed Cenozoic (mainly after 20 Ma)

54   basaltic magmatism occurred in the eastern China which is a part of East Asia

55   Cenozoic volcanism belt [e.g. *Zhou and Armstrong*, 1982; *Miyashiro*, 1986]. Although

56   the genesis of these intraplate basalts is still debated [*Chen et al.*, 2007; *Zou et al.*,

57   2008; *Richard and Iwamori*, 2010], the effect from the subducting Pacific plate is

58   expected.

59   The Subei basin in the eastern China (Figure 1) is close to the Dabie ultra-pressure

60   metamorphic belt which was created by the Triassic collision between the South

61   China block and the North China block [*Li et al.*, 1993], and is a suitable area to study

62   the potential influence of the subducted oceanic and continental plates. In this paper,

63   we carried out oxygen isotope analysis for peridotite xenoliths from the Subei basin to

64   trace the recycled crustal signatures in the upper mantle of eastern China.

65   **2. SAMPLES AND RESULTS**

66   Cenozoic basaltic volcanoes are widely distributed in the Subei basin (Figure 1)

67   and many of them contain peridotite xenoliths. 28 peridotite samples used in this

68   paper are from Panshishan (10 samples), Lianshan (7 samples) and Fangshan (11

69   samples); the K-Ar age of Fangshan basalt is ~9 Ma [*Chen and Peng*, 1988]. Most

70   xenoliths are spinel lherzolites with only one harzburgite (sample PSS17 from

71   Panshishan). Textures vary from coarse-grained protogranular (~70% of total samples)

72   through porphyroclastic (~20%) to equigranular (~10%) and no hydrous phases were

73   observed. The calculated equilibrium temperatures are from ~900°C to ~1,200°C

74   (Table 1). The major element and H_2O contents of peridotite minerals have been

75   reported by *Bonadiman et al*. [2009] and *Xia et al*. [2010].

76   Oxygen isotope compositions for minerals from 28 peridotites are given in Table 1

77   and shown in Figure 2. Mineral $\delta^{18}O$ values show large variations: ol=5.02‰ to

78   5.98‰ (average=5.50‰, 1σ=0.24, n=28), opx=5.46‰ to 6.78‰ (average =6.09‰,

79   1σ=0.31, n=27), and cpx=4.74‰ to 6.31‰ (average =5.62‰, 1σ=0.39, n=28). The

80   range of three localities is overlapped except Lianshan opx exhibit some higher $\delta^{18}O$

81   values. In addition, the oxygen isotope fractionations between coexisting mineral

82   phases ($\Delta^{18}O_{a-b}=\delta^{18}O_a-\delta^{18}O_b$) are notable: $\Delta^{18}O_{opx-ol}$= -0.46‰ to 1.26‰ and $\Delta^{18}O_{cpx-ol}$

83   = -0.65‰ to 0.97‰.

84

85   **3. DISCUSSION**

86   Peridotite xenoliths hosted by alkali basalts are direct samples of the continental

87   lithospheric mantle. They largely preserve the geochemical signatures of the mantle

88   source due to the rapid ascent to the surface (generally within a maximum of 50 hours

89   after their entrainment in the host magma, *O'Reilly and Griffin*, [2010]) and "quench"

90   effect response to sudden temperature decrease at the surface. In addition, we only

91   measured the fresh interior of minerals devoid of interaction with host magma. Our

92   data therefore can be used to directly infer their mantle source message.

93   *Mattey et al*. [1994] measured 27 spinel peridotites of the worldwide, and the

94   average $\delta^{18}O$ values of ol, opx and cpx are 5.12‰, 5.70‰ and 5.55‰, respectively.

95   Not only the ol, opx and cpx display equilibrium fractionations under lithospheric

96   mantle temperatures (900-1200°C), but also the ol value is in agreement with that of

97   the ol phenocrysts (~5.2‰) in MORBs [*Eiler et al.*, 2000], these values are generally

98   accepted as the "normal" mantle values. Compared to the dataset of *Mattey et al.*

99   [1994] the Subei basin peridotite minerals show a larger range, and typically ol and

100   opx have higher $\delta^{18}O$ values and cpx $\delta^{18}O$ values are either higher or lower than the

101   "normal" mantle values. Under lithospheric mantle temperatures (900-1200°C), the

102   fractionation of oxygen isotope between opx and cpx should be little and order of ^{18}O

103   enrichment should be opx>cpx>ol [*Chiba et al.* 1989]. The results of experiments

104   [*Chiba et al.* 1989; *Rosenbaum et al.* 1994a] and theoretical calculations [*Zheng et al.*

105   1993] show that $\Delta^{18}O_{opx-ol}$ is generally > 0.5‰ and $\Delta^{18}O_{cpx-ol}$ >0.4‰. As to the Subei

106   basin peridotites, $\Delta^{18}O_{opx-ol}$ is -0.46‰~1.26‰ and $\Delta^{18}O_{cpx-ol}$ is -0.65‰~0.97‰

107   (Figure 2); the smaller even negative fractionations cannot be achieved by close

108   system equilibrium. Thus, both the observed higher and lower $\delta^{18}O$ value of the Subei

109   peridotite minerals than those of the "normal" mantle and the disequilibrium

110   fractionations between ol and pyroxenes require crust-derived fluids involved in the

111   mantle metasomatism events.

112   The high $\delta^{18}O$ value for ol and opx and low $\delta^{18}O$ values for cpx and disequilibrium

113   fractionations among them are not likely to be the result of selective interaction of the

114   fluids with different $\delta^{18}O$ values during a single metasomatic event, so separate events

115   involving different fluids with either high or low $\delta^{18}O$ values are needed. Take the

116   considerations below: (1) oxygen isotope diffusivity of ol is ~2 orders of magnitude

117   slower than pyroxene [*Chiba et al.* 1989; *Farver*, 1989; *Rosenbaum et al.* 1994b], (2)

118   different grain sizes (ol≥opx>cpx); and (3) mineral modal abundance (ol>opx>cpx) in

119   peridotite xenoliths, the $\delta^{18}O$ values of cpx would change more rapid than ol and opx

120   upon to metasomatic events, thus the metasomatic event with low $\delta^{18}O$ values fluids

121   should be after that with high $\delta^{18}O$ values fluids.

122   So, a two-stage metasomatism model is proposed here to explain the Subei

123   peridotite data. The high $\delta^{18}O$ value fluids were involved in the first metasomatism

124   event and interacted with ol, opx and cpx to introduce ^{18}O enrichment for them due to

125   a large amount of fluids and sufficient time. The sample with highest $\delta^{18}O$ values is

126   LS05 in which ol, opx and cpx $\delta^{18}O$ values are 5.69‰, 6.78‰ and 5.91‰

127   respectively, the fluids therefore should have $\delta^{18}O$ values > 7‰ which is much higher

128   than the normal mantle fluids [5.7±0.3‰, *Eiler et al.*, 2000] The second

129   metasomatism event should involve low $\delta^{18}O$ fluids. The lowest $\delta^{18}O$ value of Subei

130   basin cpx is 4.37‰ (FS14) and this peridotite also displays negative $\Delta^{18}O_{cpx-ol}$ of

131   -0.65‰. If we assume the primary $\Delta^{18}O_{cpx-ol}$ of FS14 is 0.4‰, to change $\Delta^{18}O_{cpx-ol}$ to

132   -0.65‰ the $\delta^{18}O$ value of the metasomatic fluids should be much less than 4.37‰

133   which is much lower than the normal mantle fluids [*Eiler et al.*, 2000]. Olivine may

134   keep the $\delta^{18}O$ value inherited from the first metasomatism event due to the slower

135   oxygen diffusivity, larger grain size and possibly a relative small amount of fluids and

136   short time, so pyroxene show disequilibrium fractionations with ol. Due to the similar

137   reasons the $\Delta^{18}O_{cpx-ol}$ value would change to larger scale than $\Delta^{18}O_{opx-ol}$ value, so

138   present more negative fractionation. These preferential metasomatic alterations with

139   pyroxenes and resulted larger variability in pyroxene $\delta^{18}O$ values have been noted in

140   lherzolites [*Mattey et al.*, 1994; *Perkins et al.*, 2006] and eclogite xenoliths [*Deines*

141   *and Haggerty*, 2000]. The scatter $\delta^{18}O$ values for the cpx in the xenoliths suggest

142   variable fluid-rock ratios, and/or varying degrees of re-equilibration with the

143   infiltrating fluids.

144   The fluids with high or low $\delta^{18}O$ values may be from either subducted continental

145   crust or oceanic crust, both of them can achieve higher and/or lower $\delta^{18}O$ values than

146   "normal" mantle due to the near-surface water-rock interactions and the magnitude of

147   deviation is depend on water-rock ratios and temperatures [*Muehlenbachs*, 1986;

148   *Zheng et al.*, 2003]. Based on the tectonic environment of the Subei basin, there are

149   three possible sources for the recycled crust-derived fluids: (1) the subducted oceanic

150   crust before the collision between the South China block with the North China block,

151   (2) the subducted continental crust during the collision between the South China block

152   with the North China block, and (3) the oceanic crust of the continuously subducting

153   Pacific plate from Mesozoic time.

154   The oxygen diffusion of oxygen in olivine and pyroxenes at mantle temperatures is

155   sufficiently rapid at the order of 10^{-19}~10^{-21} m^2/s [*Farver*, 1989; *Ryerson et al.*, 1989;

156   *Ingrin et al.*, 2001]. *Gregory and Taylor* [1986] suggested that the disequilibrium

157   effects would disappear in a few tens of millions of years or less at mantle

158   temperatures. In the case of Subei peridotite, Negative disequilibrium fractionation

159   exists in less than 10Ma at mantle condition (See detail calculation in supplementary).

160   Therefore, considering that the xenoliths were entrained and brought to surface by

161   the ~9Ma Subei basin basalts, the metasomatic events likely occurred within the last

162   100 Ma. The peak time of the collision between the South China block and the North

163   China block is ~230 Ma [*Li et al.*, 1993], thus neither the subducted oceanic crust

164   before the collision nor the subducted continental crust during the collision can

165   account for the oxygen isotope disequilibrium. The best candidate is the oceanic crust

166   of the continuously subducting Pacific plate from Mesozoic time.

167   The extremely large variations in the (La/Yb)n ratios of the clinopyroxenes from

168   the Subei basin peridotite and the absence of correlations between oxygen isotope

169   fractionation among minerals and mineral modes (Figure 3) and (La/Yb)n (Figure 4)

170   support a multi-stage metasomatic overprint, involving LREE-enriched fluids from

171   subducted material bearing different oxygen isotopic ratios.

172   4.   CONCLUDING REMARKS

173   Oxygen isotopic compositions of the Subei basin peridotite xenoliths are

174   characterized by (1) ol and opx have $\delta^{18}O$ values higher and cpx lower than that of

175   "normal" mantle, and (2) coexisting minerals exhibit disequilibrium fractionations

176   with $\Delta^{18}O_{cpx-ol}$ down to -0.65‰. These characteristics cannot be from metasomatism

177   induced by mantle fluids, but by crustal fluids. Because the high $\delta^{18}O$ values for ol

178   and opx and low values for cpx is not likely to be the result of selective interactions

179   with the fluids having different $\delta^{18}O$ values during a single metasomatic event,

180   separate fluids with high and low $\delta^{18}O$ values respectively are needed. Thus we

181   propose a two-stage metasomatic modal: high $\delta^{18}O$ fluids interacted with the

182   peridotites at the first stage and low $\delta^{18}O$ fluids at the second stage. The negative

183     $\Delta^{18}O_{cpx\text{-}ol}$ values cannot be preserved for more than ~100 Ma years under mantle

184   conditions, so at least the metasomatism involving low $\delta^{18}O$ fluids should be very

185   recent before the basaltic eruption (~9 Ma). Considering the geological environment

186   of the Subei basin, the subducting Pacific plate is the best candidate to provide such

187   fluids.

188   **ACKNOWLEDGMENTS**

189   **REFERENCES CITED**

190 Bonadiman, C., Y.T. Hao, M. Coltorti, L. Dallai, and B. Faccini (2009), Water contents of
191   pyroxenes in intraplate lithospheric mantle, *European Journal of Mineralogy*, 21,
192   637-647.

193 Chen, D.G., and Z.C. Peng (1988), K–Ar ages and Pb, Sr isotopic characteristics of some
194   Cenozoic volcanic rocks from Anhui and Jiangsu Provinces China, *Acta Petrologica Sinica*,
195   2, 12-16 (in Chinese with English abstract).

196 Chen, Y., Y. Zhang, D. Graham, S. Su, snd J, Deng (2007), Geochemistry of Cenozoic basalts and
197   mantle xenoliths in Northeast China, *Lithos*, 96, 108-126.

198 Chiba, H., T. Chacko, R. Clayton, and J. Goldsmith (1989), Oxygen isotope fractionations
199   involving diopside, forsterite, magnetite, and calcite, application to geothermometry,
200   *Geochimica et Cosmochimica Acta*, 53, 2985–2995.

201 Choi, S.H., S.B. Mukasa, X.H. Zhou, X.H. Xian, and A.V. Andronikov (2008), Mantle dynamics
202   beneath East Asia constrined by Sr, Nd, Pb and Hf isotopic systematics of ultramafic
203   xenoliths and their host basalts from Hannuoba, North China, *Chemical Geology*, 248, 40-61.

204 Deines, P., and S. Haggerty (2000), Small-scale oxygen isotope variations and petrochemistry of
205   ultradeep (>300 km) and transition zone xenoliths, *Geochimica et Cosmochimica Acta*, 64,
206   117–131.

207 Eiler, J. M., P. Schiano, N. Kitchen, and E.M. Stopler (2000), Oxygen-isotope evidence for
208   recycled crust in the sources of mid-ocean-ridge basalts, *Nature*, 403, 530-534.

209 Farver, J.R., (1989), Oxygen self-diffusion in diopside with application to cooling rate
210   determinations, *Earth and Planetary Science Letters*, 92, 86–396.

211 Gregory, R.T., and H.P. Taylor (1986), Non-equilibrium, metasomatic $^{18}O/^{16}O$ effects in upper
212   mantle mineral assemblages, *Contributions to Mineralogy and Petrology*, 93, 124-135.

213 Ingrin, J., L. Pacaud, and O. Jaoul (2001), Anisotropy of oxygen diffusion in diopside, *Earth and*
214   *Planetary Science Letters*, 192, 347–361, doi,10.1016/S0012-821X[01]00460-5.

215 Kuritani, T., E. Ohtani, and J. Kimura (2011), Intensive hydration of the mantle transition zone
216   beneath China caused by ancient slab stagnation, *Nature Geoscience*, 4, 713-716.

217 Li S.G., Y.L. Xiao, D.L. Liou, Y.Z. Chen, N.J. Ge, Z.Q. Zhang, S.S. Sun, B.L. Cong, R.Y. Zhang,

218   S.R. Hart, and S.S. Wang (1993), Collision of the North China and Yangtse Blocks and
219   formation of coesite-bearing eclogites, Timing and processes, *Chemical Geology*, 109,
220   89-111.

221 Mattey, D., D. Lowry, and C. Macpherson (1994), Oxygen isotope composition of mantle
222   peridotite, *Earth and Planetary Science Letters*, 128, 231–241.

223 Miyashiro, A. (1986), Hot region and the origin of marginal basins in the western Pacific,
224   *Tectonophysics*, 339, 385-401.

225 Muehlenbachs, K. (1986), Alteration of the oceanic crust and ^{18}O history of seawater, in *Stable
226   isotopes in high-temperature geologic processes*, vol. 16, edited by J.W. Valley et al., pp.
227   425-444, Mineral Soc Amer Reviews in Mineralogy, Washington D.C.

228 O'Reilly, S.Y., and W.L. Griffin (2010), Rates of magma ascent, constraints from mantle-derived
229   Xenoliths, *in Timescales of magmatic processes, from core to atmosphere*, edited by A.
230   Dossetoet al., John Wiley & Sons, Ltd, Chichester, UK.

231 Perkins, G.B., Z.D. Sharp, and J. Selverstone (2006), Oxygen isotope evidence for subduction and
232   rift-related mantle metasomatism beneath the Colorado Plateau–Rio Grande rift transition,
233   *Contributions to Mineralogy and Petrology*, 151, 633-650.

234 Richard, G.C., and H. Iwamori (2010), Stagnant slab, wet plumes and Cenozoic volcanism in East
235   Asia, *Physics of the Earth and Planetary Interiors*, 183, 280-287.

236 Rosenbaum, J.M., T.K. Kyser, and D. Walker (1994a), High-temperature oxygen-isotope
237   fractionation in the enstatite-BaCO$_3$ system, *Geochim Cosmochim Acta*, 58, 2653–2660.

238 Rosenbaum, J.M., D. Walker, and T.K. Kyser (1994b), Oxygen isotope fractionation in the mantle,
239   *Geochimica et Cosmochimica Acta*,   58, 4767–4777.

240 Ryerson, F.J., W.B. Durham, D.J. Cherniak, and W.A. Lanford (1989), Oxygen diffusion in olivine,
241   effect of oxygen fugacity and implications for creep, *Journal of Geophysical Research*, 94,
242   4105–4118.

243 Su, B.X., H.F. Zhang, E. Deloule, A. Sakyi, Y. Xiao, Y.J. Tang, Y. Hu, J.F. Ying, and P. Liu
244   (2011), Extremely high Li and low δ^7Li signatures in the lithospheric mantle, *Chemical
245   Geology*, 292-293, 149-157. doi, 10.1016/j.chemgeo.2011.11.023.

246 Stolper, E., and S. Newman (1994), The role of water in the petrogenesis of Mariana trough
247   magmas, *Earth and Planetary Science Letters*, 121, 293-325.

248 Tang, Y.J., H.F.Zhang, E. Nakamura, and J.F. Ying (2011), Multistage melt/fluid-peridotite
249   interactions in the refertilized lithospheric mantle beneath the North China Craton,
250   constraints from the Li-Sr-Nd isotopic disequilibrium between minerals of peridotite
251   xenoltihs, *Contributions to Mineralogy and Petrology*, 161, 845-861.

252 Tatsumoto, M., A.R. Basu, W.K. Huang, J.W. Wang, and G.H. Xie (1992), Sr, Nd and Pb isotopes
253   of ultramafic xenoliths in volcanic rocks of eastern China, enriched components EMI and
254   EMII in subcontinental lithosphere, *Earth and Planetary Science Letters*, 113, 107-128.

255 Windley, B.F., S. Maruyama, and W.J. Xiao (2010), Delamination/thinning of sub-continental
256   lithospheric mantle under eastern China, the role of water and multiple subduction, *American
257   Journal of Science*, 310, 1250-1293,

258 Wu, F.Y., R.J. Walker, Y.H. Yang, H.L. Yuan, and J.H. Yang (2006), The chemical-temporal
259   evolution of lithospheric mantle underlying the North China Craton, *Geochimica et
260   Cosmochimica Acta*, 70, 5013-5034.

261   Xia, Q.K., L. Dallai, and E. Deloule (2004), Oxygen and hydrogen isotope heterogeneity of
262   clinopyroxene megacrysts from Nushan Volcano, SE China, *Chemical Geology*, 209,
263   137-151.

264   Xia, Q.K., Y.T. Hao, P. Li, E. Deloule, M. Colotori, L. Dallai, X.Z. Yang, and M. Feng (2010),
265   Low water content of the Cenozoic lithospheric mantle beneath the eastern part of the North
266   China Craton, *Journal of Geophysical Research*, 115, B07207, doi,10.1029/2009JB006694.

267   Xu, Y.G, M.Z. Menizies, D. Mattey, D. Lowry, B. Harte, and R.W. Hinton (1996), The nature of
268   the lithospheric mantle near the Tancheng-Lujiang fault, China, an integration of texture,
269   chemistry and O-isotopes, *Chemical Geology*, 134, 67-81.

270   Xu, Y.G. (2001), Thermo-tectonic destruction of the Archean lithospheric keel beneath the
271   Sino-Korean craton in China, evidence, timing and mechanism, *Physics and Chemistry of the
272   Earth*, 26A, 747-757.

273   Xu, X.S., S.Y. O'Reilly, W.L. Griffin, and X.M. Zhou (2000), Genesis of young lithospheric
274   mantle in southeastern China, a LAM-ICPMS trace element study, *Journal of Petrology*, 41,
275   111-148.

276   Zhang, H.F. (2005), Transformation of lithospheric mantle through peridotite-melt reaction, a case
277   of Sino-Korean craton, *Earth and Planetary Science Letters*, 237, 768-780.

278   Zheng, J.P., S.Y. O'Reilly, W.L. Griffin, F.X. Lu, and M. Zhang, (1998), Nature and evolution of
279   Cenozoic lithospheric mantle beneath Shandong Peninsula, Sino-Korea craton, eastern China,
280   *International Geology Review*, 40, 471-499.

281   Zheng, J.P., W.L. Griffin, S.Y. O'Reilly, J.S. Yang, T.F. Li, M. Zhang, R.Y. Zhang, and J.G. Liou
282   (2006), Mineral chemistry of peridotites from Paleozoic, Mesozoic and Cenozoic lithosphere,
283   constraints on mantle evolution beneath eastern China, *Journal of Petrology*, 47, 2233-2256.

284   Zheng, Y.F. (1993), Calculation of oxygen isotope fractionation in anhydrous silicate minerals,
285   *Geochimica et Cosmochimica Acta*, 57, 1079-1091.

286   Zheng, Y.F., B. Fu, B. Gong, and L. Li (2003), Stable isotope geochemistry of ultrahigh pressure
287   metamorphic rocks from the Dabie-Sulu orogen in China, implications for geodynamics and
288   fluid regime, *Earth-Science Reviews*, 62, 105-161.

289   Zhou, X.H., and R. Armstrong (1982), Cenozoic volcanic-rocks of eastern China-secular and
290   geographic trends in chemistry and strontium isotopic composition, *Earth and Planetary
291   Science Letters*, 58, 301-329.

292   Zou, H.B., Q.C. Fan, and Y.P. Yao (2008), U-Th systematic of dispersed young volcanoes in NE
293   China, Asthenosphere upwelling caused by piling up and upward thickening of stagnant
294   Pacific slab, *Chemical Geology*, 255, 134-142.

295

FIGURE CAPTIONS

Figure 1. Simplified tectonic units of Eastern China and sample locality in Subei

    basin.

Figure 2. Oxygen isotope compositions of the peridotite minerals of the Subei basin. **a**
    Orthopyroxene versus olivine, **b** clinopyroxene versus olivine. PSS:
    Panshishan, LS: Lianshan, FS: Fangshan. Oxygen isotope equilibrium at
    temperatures of 900 and 1200°C has been calculated on the basis of their
    fractionation values [Chiba et al., 1989; Zheng, 1993]. Cross line represents
    the analytical uncertainty on the replicate analyses [±0.15‰]. Shadow area
    is the range of global spinel peridotites [Mattey et al. 1994].

Figure 3. The correlation between oxygen isotope compositions and mode
    composition of peridotite minerals of the Subei basin. **a** olivine, **b**
    orthopyroxene, **c** clinopyroxene.

Figure 4. Clinopyroxene $\delta^{18}O$ value vs. (La/Yb)n. n indicate normalized to C1-chondrtie
    value of Sun and Mcdonough[1989]

SFigure 1. Rear Earth Element of clinopyroxene of Subei basin peridotite.

314   Table 1 Oxygen isotope composition of peridotite minerals from Subei basin

Sample	δ18O SMOW (‰)			Δ18O a-b (‰)			Mode(%) point counting				T(℃)[a]	Mg# cpx[b]	(La/Yb)n[c]
	ol	opx	cpx	Δopx-ol	Δcpx-ol	Δcpx-opx	ol	opx	cpx	sp			
PSS01	5.71	6.24	5.31	0.53	-0.40	0.93	71	18	10	1	960	91.32	0.28
PSS02	5.46	5.69	5.38	0.23	-0.08	0.31	65	20	15	1	956	91.15	4.64
PSS05	5.47	6.34	5.67	0.87	0.20	0.67	62	20	12	2	964	92.36	0.81
PSS11	5.59	6.20	5.83	0.61	0.24	0.37	57	29	12	2	888	91.65	0.87
PSS12	5.30	5.67	5.31	0.37	0.01	0.36	58	24	15	1	957	92.36	0.34
PSS13	5.20	5.84	5.23	0.64	0.03	0.61	65	20	13	2	966	92.46	0.43
PSS15	5.49	6.03	5.37	0.54	-0.12	0.66	62	26	13	2	902	91.89	0.64
PSS16	5.46	6.01	5.18	0.55	-0.28	0.83	50	33	16	1	961	89.17	0.41
PSS17	5.45	6.36	5.66	0.91	0.21	0.70	75	18	5	2	953	92.84	1.07
PSS19	5.38	5.91	5.23	0.53	-0.15	0.68	70	16	13	1	959	92.36	0.54
LS05	5.69	6.78	5.91	1.09	0.22	0.87	60	28	10	2	904	91.62	0.04
LS06	5.90	6.36	6.15	0.46	0.25	0.21	66	23	10	1	972	91.31	0.49
LS12	5.34	6.50	6.01	1.16	0.67	0.49	72	16	9	3	954	92.94	0.22
LS17	5.30	6.23	5.95	0.93	0.65	0.28	73	17	7	1	972	93.46	13.76
LS20	5.98	6.57	6.03	0.59	0.05	0.54	78	10	10	2	966	91.36	4.56
LS22	5.56	6.35	5.97	0.79	0.41	0.38	64	22	12	2	914	91.03	1.19
LS31	5.10	6.36	6.07	1.26	0.97	0.29	68	15	17	1	893	91.08	0.11
FS01	5.71	6.07	5.87	0.36	0.16	0.20	53	27	18	2	972	91.32	3.92
FS03	5.25	6.07	5.06	0.82	-0.19	1.01	58	27	13	2	1191	90.48	0.16
FS07	5.54	5.80	5.71	0.26	0.17	0.09	57	28	12	3	1001	90.51	0.21
FS12	5.71	5.59	5.63	-0.12	-0.08	-0.04	61	30	7	2	1063	90.39	0.21
FS14	5.02	4.74	4.37	-0.28	-0.65	0.37	66	20	11	3	1063	89.20	3.55
FS16	5.26	5.98	5.46	0.72	0.20	0.52	76	17	6	1	1023	91.50	16.22
FS17	5.67	6.03	6.31	0.36	0.64	-0.28	56	26	16	2	972	91.40	1.39
FS19	5.64	6.13	5.46	0.49	-0.19	0.68	58	25	14	3	1113	88.64	1.37
FS23	5.37	5.82	5.80	0.45	0.43	0.02	71	15	12	2	1094	90.09	2.42
FS26	5.44	6.05	5.87	0.61	0.43	0.18	70	20	9	1	967	90.89	0.37

315

316   a Temperature calculated with Ca-in opx thermometry and from Xia et al.[2010]

317   b Mg#=100*Mg/(Mg+Fe)

318   c n indicate normalized to C1-chondrtie value of Sun and Mcdonough[1989]

319

320   STable 1 Rear Earth Elements of clinopyroxene of Subei basin peridotite

| Sample	La	Ce	Pr	Nd	Sm	Eu	Gd	Tb	Dy	Ho	Er	Tm	Yb	Lu
PSS01	0.78	2.53	0.50	3.07	1.36	0.63	2.36	0.48	3.29	0.72	2.04	0.30	2.06	0.30
PSS02	9.66	19.93	2.27	9.16	1.88	0.76	2.40	0.43	2.63	0.59	1.58	0.22	1.56	0.22
PSS05	2.06	5.01	0.76	4.11	1.51	0.66	2.37	0.44	3.10	0.70	1.86	0.28	1.86	0.27
PSS11	2.06	6.15	1.05	6.22	2.25	0.95	3.21	0.54	3.61	0.75	1.98	0.27	1.85	0.25
PSS12	0.91	3.27	0.63	4.10	1.75	0.73	2.47	0.46	3.16	0.72	2.06	0.30	1.88	0.29
PSS13	0.87	2.25	0.35	1.97	0.84	0.36	1.52	0.31	2.16	0.52	1.54	0.21	1.47	0.22
PSS15	1.76	5.48	0.97	5.83	2.20	0.88	3.04	0.52	3.45	0.80	2.17	0.30	2.00	0.29
PSS16	1.08	3.86	0.72	4.55	1.83	0.76	2.73	0.52	3.49	0.75	2.03	0.30	1.93	0.28
PSS17	1.33	3.97	0.60	3.04	0.83	0.30	0.94	0.18	1.31	0.30	0.94	0.14	0.96	0.13
PSS19	0.80	2.62	0.38	1.92	0.77	0.56	1.42	0.29	2.00	0.44	1.22	0.17	1.13	0.16
LS05	0.12	0.88	0.27	2.19	1.25	0.57	2.27	0.45	3.18	0.73	2.06	0.30	2.04	0.28
LS06	1.13	4.08	0.71	4.26	1.77	0.67	2.39	0.44	3.09	0.68	1.81	0.27	1.74	0.25
LS12	0.27	0.97	0.19	1.16	0.49	0.21	0.93	0.19	1.43	0.33	1.00	0.15	0.96	0.13
LS17	10.81	13.17	1.37	5.20	0.72	0.18	0.60	0.09	0.60	0.13	0.37	0.06	0.51	0.08
LS20	8.98	20.80	2.70	12.28	2.94	1.05	2.92	0.49	2.85	0.58	1.45	0.21	1.46	0.21
LS22	3.24	10.36	1.76	9.55	2.92	1.10	3.53	0.58	3.72	0.79	2.14	0.30	1.98	0.29
LS31	0.33	1.77	0.43	3.30	1.58	0.73	2.76	0.50	3.61	0.81	2.21	0.33	2.22	0.32
FS01	7.32	13.28	1.40	5.84	1.58	0.60	2.18	0.38	2.58	0.54	1.47	0.21	1.37	0.20
FS03	0.24	0.99	0.21	1.43	0.75	0.35	1.36	0.29	1.92	0.45	1.18	0.17	1.11	0.16
FS07	0.50	2.12	0.45	2.99	1.44	0.59	2.29	0.46	3.08	0.67	1.89	0.27	1.82	0.26
FS12	0.45	1.43	0.29	1.97	1.04	0.44	1.80	0.35	2.40	0.54	1.61	0.22	1.52	0.23
FS14	7.13	8.18	1.06	5.50	1.73	0.75	2.49	0.43	2.88	0.64	1.74	0.25	1.55	0.22
FS16	16.05	25.69	2.15	7.59	1.71	0.64	1.63	0.27	1.71	0.35	0.95	0.13	0.84	0.11
FS17	2.90	4.87	0.66	3.51	1.34	0.59	2.16	0.39	2.75	0.59	1.66	0.23	1.55	0.22
FS19	2.94	4.94	0.68	4.16	1.54	0.63	2.34	0.43	2.91	0.66	1.77	0.24	1.62	0.23
FS23	3.23	4.92	0.71	4.13	1.42	0.56	1.81	0.31	1.95	0.42	1.10	0.14	0.92	0.14
FS26	0.96	3.52	0.69	4.28	1.78	0.72	2.62	0.49	3.43	0.75	2.09	0.29	1.92	0.28

321
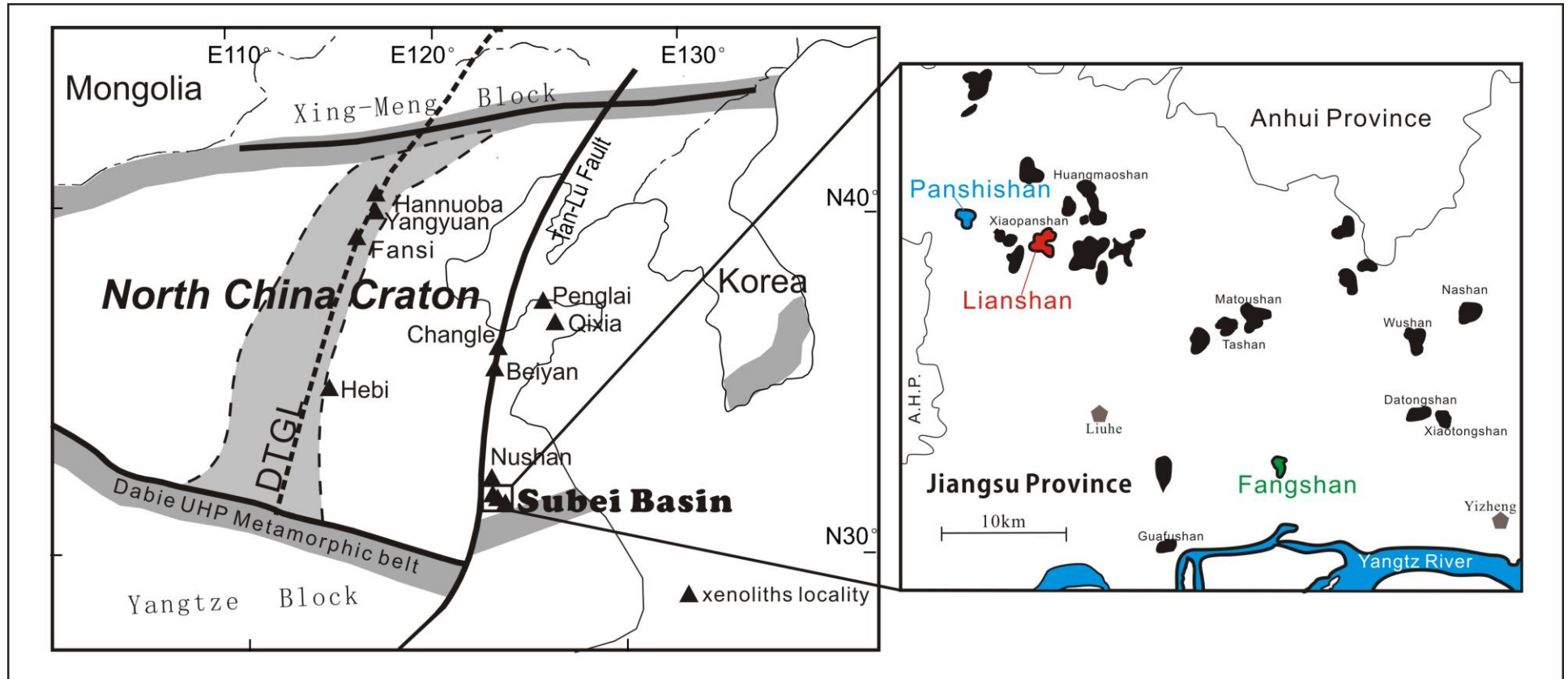
Figure 1. Simplified tectonic units of Eastern China and sample locality in Subei basin.
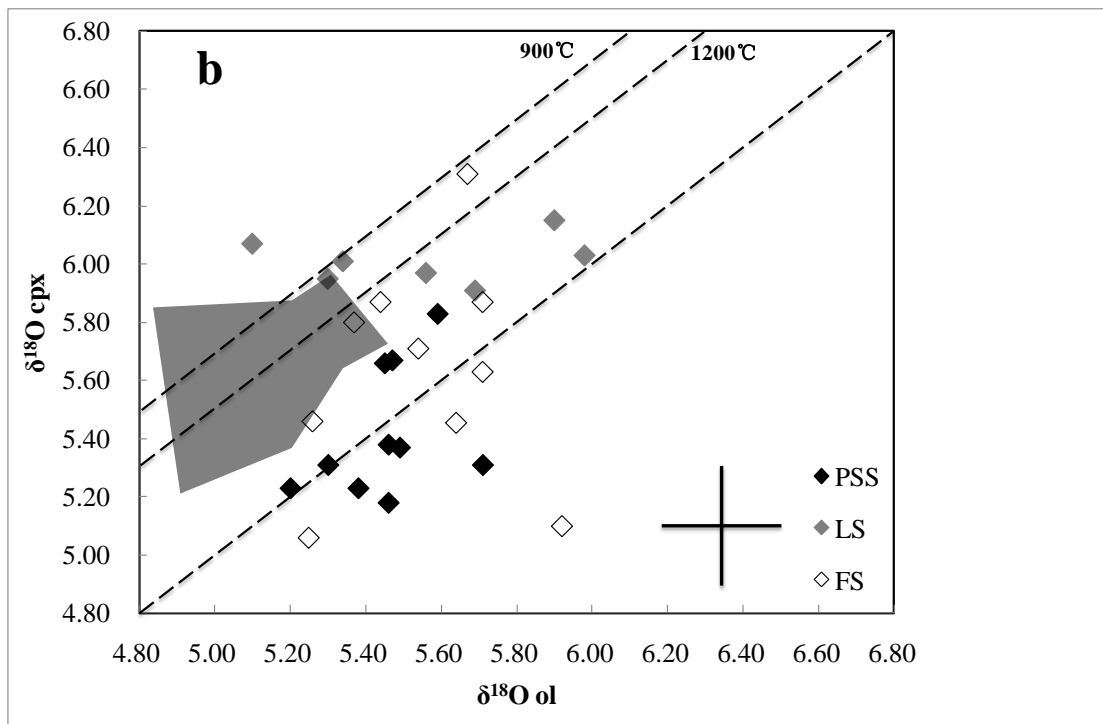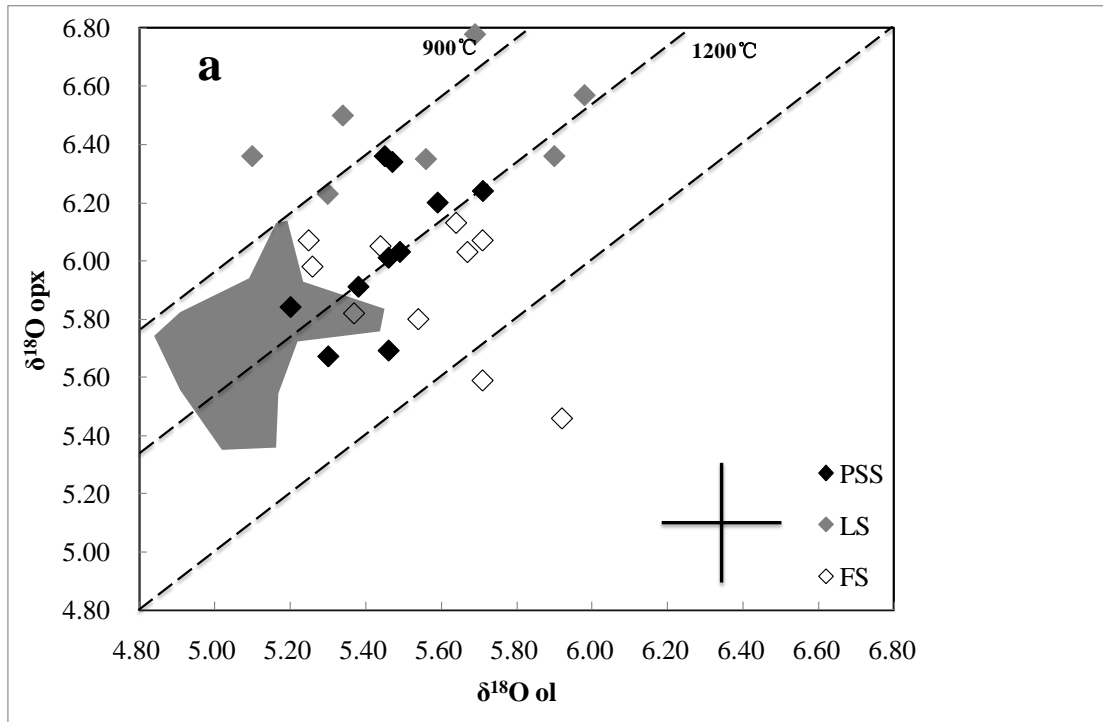
Figure 2. Oxygen isotope compositions of the peridotite minerals of the Subei basin. **A** Orthopyroxene versus olivine, **B** clinopyroxene versus olivine. PSS: Panshishan, LS: Lianshan, FS: Fangshan. Oxygen isotope equilibrium at temperatures of 900 and 1200°C has been calculated on the basis of their fractionation values [Chiba et al., 1989; Zheng, 1993]. Cross line represents the analytical uncertainty on the replicate analyses [±0.15‰]. Shadow area is the range of global spinel peridotites [Mattey et al. 1994].
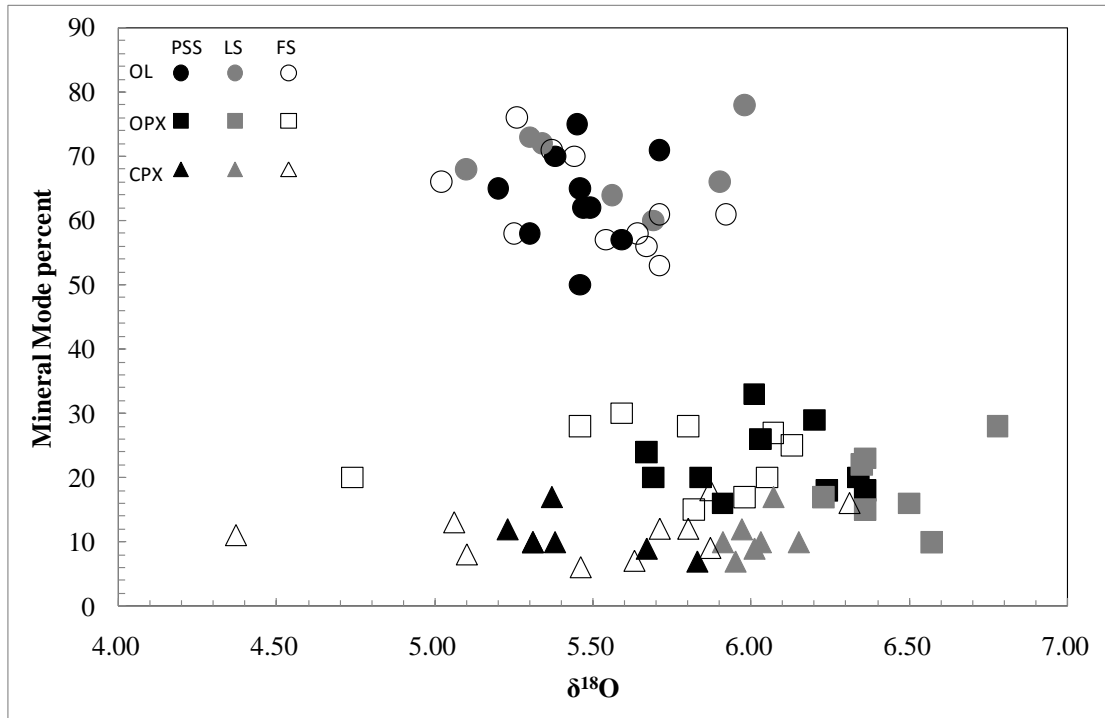
Figure 3. Oxygen isotope compositions of the peridotite minerals of the Subei basin vs. mode composition.
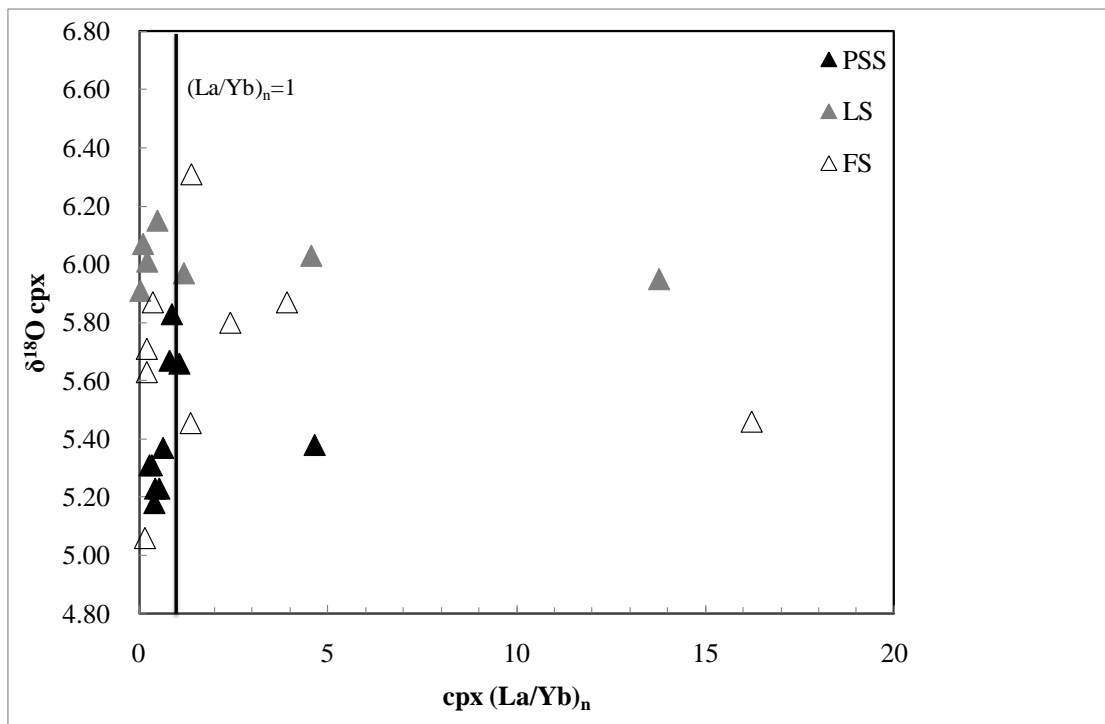
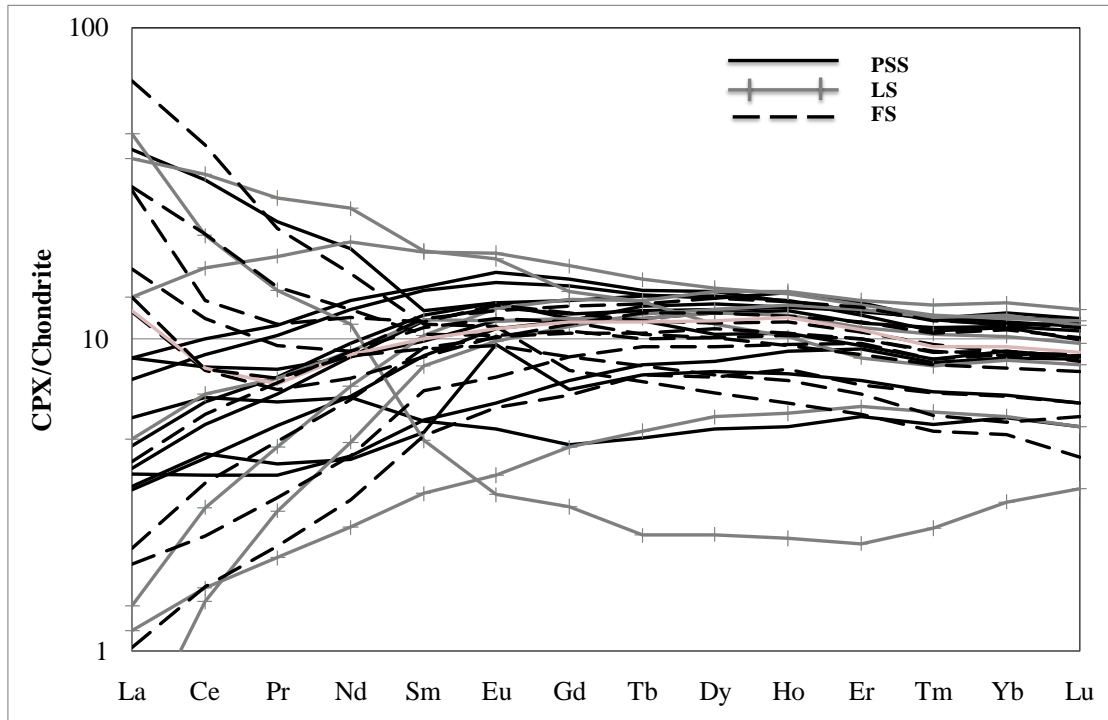Figure 4. Clinopyroxene $\delta^{18}O$ value vs. $(La/Yb)n$

SFigure 1 Rear earth element of clinopyroxene of Subei basin peridotite

Analytical method

Oxygen isotope

Oxygen isotope data were measured at the CNR-IGG of PISA by laser fluorination, reacting 1 to 1.5 mg ol, opx, cpx and sp fragments in F_2 gas atmosphere. We employed a 25 W CO_2 laser operating at a wavelength of 10.6 μm to irradiate the samples, and pure fluorine desorbed at 290°C from hexafluoropotassium-nickelate salt as a reagent. Three pre-fluorination steps were made before measuring new sets of analyses, in order to remove the moisture in the sample holder and the line. The O_2 produced during laser fluorination together with excess fluorine were passed through potassium chloride salt and excess fluorine was converted into a potassium-fluoride salt and chlorine gas. A cryogenic trap cooled at liquid nitrogen temperature was used to freeze chlorine. After purification, O_2 was trapped over a cold finger filled with 13A zeolites, and then transferred to a Finnigan Delta Plus Mass Spectrometer for oxygen isotope analysis. QMS and NBS30 standard samples were measured at the beginning of each day of analysis; after the standard samples reached the accepted values, minerals samples sequence started. 5 to 6 standards were measured during each set of analyses. The average $\delta^{18}O$ value of QMS is 14.05 ±0.17 ‰ (1 σ) and the $\delta^{18}O$ value of NBS30 is 5.24±0.15 ‰ (1 σ). All $\delta^{18}O$ values are relative to SMOW. At least two fragments were analyzed for each mineral, and the variation within the same sample is less than the precision of standards. All minerals were measured at least twice and some of them more than three times; the results demonstrated the homogeneity with no variations observed among different grains of the same mineral

of a given sample and the average value of multiple analyses is used. Some samples were cross checked at the University of New Mexico, USA and the University of Gottingen, Germany, and the results are in agreement with the Pisa lab within analytical precision.

REE

Measurements of trace element composition of Clinopyroxenes and a few Orthopyroxenes were carried out at the LA-ICPMS laboratory of the University of Science and Technology of China, Hefei (USTC). FTIR thin sections were broken and selected minerals grains were mounted in epoxy pellet and polished. Mineral grains were ablated in situ with Coherent company GeoLas pro ArF laser system with beam wavelength 193 nm at 10 Hz repetition rate and 10 J/cm2 energy per plus. The ablation crater diameters were 60μm, and the sample aerosol was carried to ICPMS by high purity Helium with flow rate of 0.3L/min. A typical analysis consists of 80-100 replicates within 80-100s. PerkinElmer DRCII ICPMS was used to analyse the aerosol samples with the RF power 1350 w and nebulized gas flow rate 0.7 L/min. The raw data were processed with LaTEcalc software. The signal intensities (counts per ppm) for each element were calibrated against the NIST 610 silicate glass standard and the ^{44}Ca content of samples was used as an internal standard. Typical analytical precision ranged from 2% to 5%.

Calculation method

In the case of Subei peridotite, Ol is modally dominant, and the $\delta^{18}O$ value of the cpx is determined using the equation of *Crank* [1975] for a semi-infinite medium

adjacent to a plane of constant composition:

$$\delta^{18}O_{cpx}(t) - \delta^{18}O_{cpx,eqm} = (\delta^{18}O_{cpx,i} - \delta^{18}O_{cpx,eqm}) \times erf(\frac{r}{2\sqrt{Dt}})$$

Where $\delta^{18}O_{cpx,eqm}$ is the $\delta^{18}O$ value of cpx in equilibrium with ol for a given temperature, $\delta^{18}O_{cpx,i}$ is the measured $\delta^{18}O$ value of cpx, r is the radius of cpx (in m), t is time (s), and D is the oxygen diffusion coefficient (m^2/s).

Parameters chosen for this calculation use the oxygen isotope results from this study, a typical cpx radius from the coarse grain xenoliths (r=1 mm), and an equilibration temperature of 1,000℃ [*Xia et al.*, 2010], which corresponds to an equilibrium $\Delta^{18}O_{cpx-ol}$=0.4‰ under mantle condition [Chiba, 1989]. Take FS14 for example, which have the lowest $\delta^{18}O$ value of cpx (4.37‰) and negative $\Delta^{18}O_{cpx-ol}$ of -0.65‰. Negative disequilibrium fractionation exists in less than 10Ma at oxygen diffusion rate of 10^{-19} m^2/s, and 100Ma at oxygen diffusion rate of 10^{-21} m^2/s).